

# Chapter 10

## Hydrochemical Insight and Groundwater Supply: A Case Study of Patagonia's Chubut River



Américo I. Torres , Luis F. H. Niencheski, Verena A. Campodonico,  
Andrea I. Pasquini, Mauricio Faleschini, and Pedro J. Depetris

**Abstract** The aim of this chapter is to assess the groundwater discharge component in the hydrological budget of NE Patagonia's Chubut River (CHR), using  $^{222}\text{Rn}$  as a quantitative groundwater tracer. The main hydrological characteristics of CHR are also presented. The annual mean discharges at Valle Inferior have decreased at a mean rate of  $10 \text{ m}^3$  per decade. Anthropogenic impacts—such as wastewater discharge—are observed in surface waters. The  $^{222}\text{Rn}$  mass balance indicated that the groundwater inflow to the CHR ranged between  $2.0$  and  $5.4 \text{ m}^3 \text{ s}^{-1}$ . Thus, such groundwater inputs may account for approximately 6–24% of the total water delivered by CHR to the SW Atlantic Ocean. However, a negative flux ( $-1.3 \text{ m}^3 \text{ s}^{-1}$ ) was recorded in another sampling site suggesting that the river is losing water to the aquifer. The nutrient fluxes toward the ocean were higher in winter than in spring. The silicic acid flux ( $1.175 \times 10^6 \text{ mol d}^{-1}$ ) was the highest, followed by the total inorganic nitrogen ( $0.08 \times 10^6 \text{ mol d}^{-1}$ ) and then by phosphorus ( $0.024 \times 10^6 \text{ mol d}^{-1}$ ). Such nitrogen flux would support a production rate of  $7.42 \times 10^6 \text{ g C d}^{-1}$ . The results presented in this study indicate that SGD represents a relevant process, which takes place in the CHR's estuarine zone.

**Keywords** Hydrology · Groundwater · Tracer · Chubut River · Patagonia

---

A. I. Torres (✉) · M. Faleschini

Laboratorio de Oceanografía Química y Contaminación de Aguas, CESIMAR, CCT  
CONICET-CENPAT, Blvd. Brown 2915 9120, Puerto Madryn, Chubut, Argentina  
e-mail: [americo@cenpat-conicet.gob.ar](mailto:americo@cenpat-conicet.gob.ar)

L. F. H. Niencheski

Instituto de Oceanografía, Fundação Universidade Federal do Rio Grande, Av. Itália km 8,  
Rio Grande, RS 96201-900, Brazil

V. A. Campodonico · A. I. Pasquini

Centro de Investigaciones en Ciencias de la Tierra, Consejo Nacional de Investigaciones  
Científicas y Técnicas y Universidad Nacional de Córdoba, Av. Vélez Sarsfield 1611,  
X5016CGA Córdoba, Argentina

P. J. Depetris

Academia Nacional de Ciencias, Avenida Vélez Sarsfield 229-249, X5000WAA Córdoba,  
Argentina

## 10.1 Introduction

The marine coastal zone receives the discharge of both rivers and groundwater. Groundwater circulating through sediment strata can crop up in a river or in the sea, through the seabed, and this event is globally identified as submarine groundwater discharge (SGD). SGD is a complex hydrological process, which is not always evident, since it can occur along the coastline, a few meters from the coast or several kilometers offshore (Bratton 2010), depending on the hydrological characteristics of the area (Kroeger and Charette 2008). The dynamics of such a complex mechanism requires a multidisciplinary approach (Burnett and Dulaiova 2003). Groundwater contributions represent a pathway of communication and exchange of chemical components between continent and sea (Moore 1999; Burnett and Dulaiova 2003). This communication path is regulated by different processes which generate a hydraulic gradient necessary to establish the water flow (Burnett et al. 2003; Santos et al. 2012). In addition, in the last decades, SGD has been considered an important source of carbon, macro- and micronutrients, heavy metals, dissolved gases and other elements, which are transferred to the marine environment (Moore 2006; Swarzenski et al. 2006). Additionally, such chemical elements can be present in high concentrations reaching up to three orders of magnitude higher than those recorded in surface water. Globally, SGD has a net flow of  $120 \times 10^{12} \text{ m}^3 \text{ y}^{-1}$  (Kwon et al. 2014), which widely exceeds the net riverine flow ( $36 \times 10^{12} \text{ m}^3 \text{ y}^{-1}$ ) toward the oceans (Milliman and Farnsworth 2011). Thus, it is evident that continental nutrient contributions can affect the biogeochemical cycles in the coastal marine zone (Garcia-Solsona et al. 2010; Godoy et al. 2013). Additionally, the contribution of essential nutrients—such as N and P—in the aquatic environment is important for the development of trophic chains but also indicates the degree of eutrophication, whereas silica may suggest coastal processes related to sediment remobilization, erosion and sedimentation, evidencing the influence of freshwater.

Studies around the world have demonstrated the effective use of geochemical tracers both to detect areas with the occurrence of SGD and to study its dynamics, as well as to estimate groundwater inflow in rivers. Among the most commonly used are radioactive isotopes, such as  $^3\text{H}$ ,  $^{219}\text{Rn}$ ,  $^{220}\text{Rn}$ ,  $^{222}\text{Rn}$ ,  $^{223}\text{Ra}$ ,  $^{224}\text{Ra}$ ,  $^{226}\text{Ra}$  and  $^{228}\text{Ra}$ , and stable isotopes, like  $^2\text{H}$ ,  $^{18}\text{O}$ ,  $\text{CFC}_s$ ,  $\text{SF}_6$  and  $^4\text{He}$  (e.g., Windom et al. 2006; Santos et al. 2009; Peterson et al. 2010; Schmidt et al. 2011; Smerdon et al. 2012; Swarzenski et al. 2017).

River waters contain low concentrations of dissolved radium and radon (Porcelli and Swarzenski 2003). Therefore, the discharge of groundwater into the deepest parts of the river channel can be detected by the characteristic radon enrichment with respect to the surface waters. Radon has a unique characteristic, because it is a noble gas and is, therefore, chemically and biologically inert. Radon is an odorless

and colorless radioactive gas that occurs naturally in air, in water and in rocks and soil. Specifically,  $^{222}\text{Rn}$  is a daughter isotope of  $^{226}\text{Ra}$  and they both reach a radioactive equilibrium over a few weeks (Cecil and Green 2000). It has been recognized as an excellent tracer to identify areas with groundwater influx (Burnett et al. 1996; Hamada 2000; Burnett and Dulaiova 2003). Likewise, it has been proved useful for estimating the infiltration of river-fed groundwater toward other aquatic environments (Macheleidt et al. 2002). The other radon isotopes ( $^{219}\text{Rn}$  and  $^{220}\text{Rn}$ ) have a half-life of less than one minute, and for this reason they are difficult to use as tracers in environmental investigations. The use of  $^{222}\text{Rn}$  as a proxy for the estimation of groundwater discharge stems from its significant concentrations in groundwater (i.e., 1000 times or more its concentration in surface water), its non-reactive nature and its short half-life ( $t_{1/2}$  3.82 days). These features make it useful in hydrological studies (Cecil and Green 2000).

In Argentina's Patagonia, there are eight rivers with Andean sources that discharge their waters into the Atlantic Ocean. They contribute nutrients, sediments, trace and major elements, which play an important role in sustaining the biological structure in Patagonia's coastal zone (Depetris et al. 2005). However, the available information on SGD in that coastal area is scarce. Preliminary results were obtained by Torres et al. (2018) who have identified the presence of SGD in the coastal areas from Patagonia, but the flows were not yet quantitatively measured. Currently, there is a lack of information regarding groundwater contribution to rivers and its interaction with surface waters. In addition, the role of SGD and the supply of nutrients in the biogeochemical cycles in the coastal zone are unknown. The goal of this study is using the activity of  $^{222}\text{Rn}$  to identify the presence of groundwater discharges in Chubut River's lower reaches, estimating the groundwater flow toward the sea. In so doing, the evaluation of the groundwater chemical contribution is sought, along with the definition of the relationship between groundwater and surface waters based on chemical and hydrological characteristics.

### 10.1.1 Study Area

The 800-km-long Chubut River crosses the homonymous province from west to east, reaching Engaño Bay, in the SW Atlantic Ocean (Fig. 10.1). Its drainage basin exceeds  $\sim 53,200 \text{ km}^2$  (Subsecretaría de Recursos Hídricos 2002), with headwaters in the Cerro de las Carreras ( $41^\circ \text{ S } 71^\circ 19' \text{ W}$ ), in Argentina's Río Negro Province, at  $\sim 1800 \text{ m}$  above sea level (a.s.l.). The main tributaries in the upper drainage are the Ñorquinco and Chico del Norte rivers, inflowing from the north, and the Tecka-Gualjaina River (i.e., drainage basin  $\sim 28,000 \text{ km}^2$ ), joining the system from the south (Fig. 10.1). Senguer-Chico del Norte River system (i.e., drainage basin of  $\sim 26,000 \text{ km}^2$ ) drains the Musters and Colhué Huapi lakes, which used to join the CHR, inflowing from the SE. Yet, due to natural obstructions that modified the original morphology, the system became endorheic.

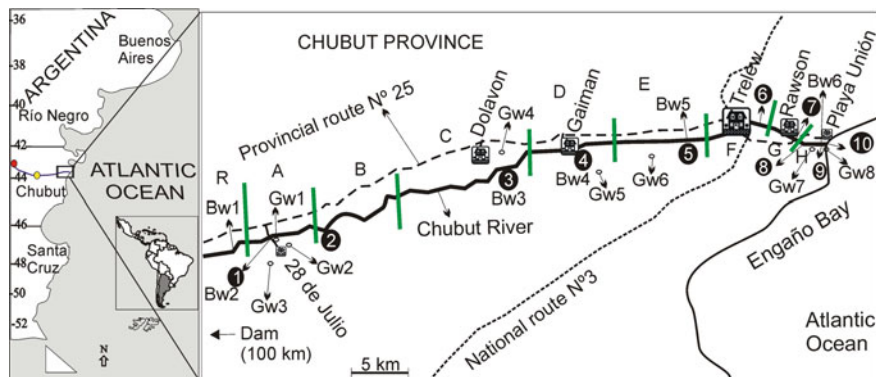


**Fig. 10.1** Study area, lower reaches of Chubut River. The sampling sites are indicated as circles (i.e., samples of surface waters, from 1 to 10); Bw, bottom water samples, and Gw, groundwater samples (i.e., from wells). Green bars correspond to box boundaries used in the estimation of mass balance calculations. Red and yellow circles are indicating the location of the El Maitén and Los Altares gauging stations, respectively

The Florentino Ameghino hydroelectric dam, located 150 km upstream from the estuary, modulates Chubut's discharges. In the Chubut's lower reach, there are two cities, Trelew (~100,000 inhabitants) and Rawson (~32,000 inhabitants). The first one has a stabilization pond system and the treated liquid is naturally evaporated and infiltrated into the soil without obvious connection with the river, while the second one discharges its urban wastewater—after receiving an activated sludge treatment—into the river. In addition, other towns (<5000 inhabitants), such as Gaiman, Dolavon and 28 de Julio, which do not have a sewage network (i.e., septic tanks, instead), are a source of diffuse infiltrations that ultimately reach the river. Furthermore, in the CHR lower basin there is an area with intensive agricultural activity, irrigated with river water, which is distributed by means of an extensive channel network. Associated with this activity, there is an intensive and uncontrolled use of fertilizers and pesticides—organochlorine and organophosphate compounds (Antolini 2012) which enter the river through unused water, diffuse flows and seepage. Additionally, there is a shallow water harbor—located only 600 m from the river mouth—which is used by boats pursuing fishing activities of high economic significance for the region. As a result of the port activities, hydrocarbons (Commendatore and Esteves 2004) and heavy metals (Gil et al. 1999) are released into the river. On several occasions, dredging of the last 600 m of the navigation channel has been made to allow the transit of medium-size fishing vessels. Furthermore, there are some fish-processing plants located on the river's margins, discharging their untreated wastewaters. The salt intrusion due to tidal effects in the estuary was observed—under low river discharge—as far as 4.5 km from the mouth (Perillo et al. 1989).

The region has an arid climate due to low rainfall (<240 mm  $y^{-1}$ ), a high rate of evapotranspiration (2000 mm  $y^{-1}$ ) and an average annual humidity of 40% (EMC

2020). These characteristics favor the strong dryness of the soil. Spring is the windy season with prevailing winds from the west to the southwest direction with an average speed of  $16.6 \text{ km h}^{-1}$  and recorded maxima of  $90 \text{ km h}^{-1}$ . The wind-borne contribution of dust to the marine environment plays a substantial role. The addition of Patagonian dust to seawater contributes nitrate and silicate nutrients, which may affect the biological productivity depending on the dust source and on the amount added (Paparazzo et al. 2018).

## 10.2 Methodology

Ten surface freshwater samples, collected between June and November 2017, were taken using a Niskin bottle in the lower course of the Chubut River. The samples were stored at  $-20 \text{ }^\circ\text{C}$  preceding the measurement of the concentrations of dissolved inorganic nutrients such as ammonium ( $\text{N-NH}_4^+$ ), nitrite and nitrate ( $\text{N-NO}_3^- + \text{NO}_2^-$ ), phosphate ( $\text{PO}_4^{3-}$ ) and silicic acid  $\text{Si(OH)}_4$  using an autoanalyzer (Skalar Analytical® V.B. 2005a, b, c). The  $\text{N-NO}_3^- + \text{NO}_2^-$  were determined together and are hereafter referred to as  $\text{N-NO}_3^-$  concentration. Ammonium concentration was determined manually according to Strickland and Parsons (1972). Furthermore, the following parameters were measured in situ: temperature, dissolved oxygen (DO), electrical conductivity (EC), pH, redox potential, total dissolved solids (TDS) and salinity using a YSI MPS 556 sensor. Also, six bottom freshwater samples were taken in November 2017. Immediately, a volume of 4 L was placed in a glass bottle to measure the  $^{222}\text{Rn}$  activity using a RAD-7 equipment (DurrIDGE Co. Inc.). The RAD-7 equipment was configured to measure the  $^{222}\text{Rn}$  activity every thirty minutes for two hours (for more details, see Campodonico et al. 2015). Another subsample was stored for the measurement of the nutrient concentrations. Additionally, groundwater samples were taken in November in seven permanent wells and in one well drilled in the beach area near the mouth of Chubut River. The physical and chemical determinations mentioned above were also carried out in groundwater samples.

The  $^{222}\text{Rn}$  activities were measured during November 2017 at 6 sampling points along the lower stretch of the CHR and on selected groundwater samples ( $n = 7$ ).  $^{222}\text{Rn}$  measurements were performed in situ by means of a RAD-7 detector (DurrIDGE Co. Inc.), a portable continuous radon-in-air monitor modified for radon-in-water that determines the activity of  $^{222}\text{Rn}$  by counting its alpha-emitting daughters ( $^{218}\text{Po}$  and/or  $^{214}\text{Po}$ ). Samples were collected in 4-L plastic bottles designed to avoid gas loss (Stringer and Burnett 2004), and  $^{222}\text{Rn}$  activity was measured in the field by means of the RAD-7, which purges  $^{222}\text{Rn}$  in water in order to achieve a rapid equilibrium of  $^{222}\text{Rn}$  between water and air.

### 10.3 Hydrological Characteristics of the Chubut River

The hydrological dynamics of the Chubut River is mainly governed by rainfall and snowfall in the upper catchments. Most of the annual discharge is delivered by the upper Chubut River (i.e., ~60–65% during the low-discharge period).

In the mountainous headwaters, atmospheric precipitations increase in May (i.e., maximum mean precipitation) and June, during the Southern Hemisphere's fall and winter, and begin a gradual decrease that reaches its minimum in November (i.e., southern spring). The uppermost Chubut River gauging station (Nacimiento, 41° 43' S, 71° 08' W)<sup>1</sup> is operative since June 1967. During a period of over 50 years (i.e., until November 2019), the maximum recorded discharge ( $Q_{\max}$ ) was  $29.17 \text{ m}^3 \text{ s}^{-1}$ , whereas the minimum ( $Q_{\min}$ ) was  $0.41 \text{ m}^3 \text{ s}^{-1}$ .

Discharge data are usually asymmetrically distributed and often adjust to a log-normal statistical distribution. Therefore, the mathematical expectation is better approached by using the geometric mean discharge ( $Q_g$ ) (e.g., Davis 1986).  $Q_g$  and the corresponding geometric standard deviation ( $S_g$ ) for the analyzed period were  $4.8 \pm 0.91 \text{ m}^3 \text{ s}^{-1}$ . The highest discharges are usually recorded in July–August, due to rainfall and snowfall, and in October–November, as a result of snowmelt.

Atmospheric precipitations at the El Maitén gauging station (42° 06' S, 71° 10' W) follow a pattern analogous to the one recorded at Nacimiento station, although maximum mean precipitation occurs in June, with the minimum also in November. Figure 10.2 shows the significant log-normal distribution exhibited by instantaneous discharges recorded at El Maitén during the 2000–2020 record period. The station is located at ~720 m a.s.l., and the available discharge time series for the period 1953–2019 includes over 6800 instantaneous discharge measurements, with  $Q_{\max} \approx 240 \text{ m}^3 \text{ s}^{-1}$  and  $Q_{\min} \approx 1.9 \text{ m}^3 \text{ s}^{-1}$ .  $Q_g$  and the corresponding  $S_g$  are  $16.2 \pm 2.23 \text{ m}^3 \text{ s}^{-1}$ . Therefore, from a statistical point of view, 95 per cent of the assembled data are comprised within  $Q_g \pm 2S_g$ :  $11.7 \text{ m}^3 \text{ s}^{-1} < Q_g < 20.7 \text{ m}^3 \text{ s}^{-1}$ .

The Los Altares gauging station is placed in a semiarid region, about 230 km west of the city of Trelew and 323 km east of city of Esquel, on the southern margin of the Chubut River. The wild landscape is known for its high cliffs and remarkable morphology. The Los Altares station (43° 53' 18.17" S, 68° 23' 57.81" W) is active since January 1943, record-keeping instantaneous discharges and other hydrometeorological variables. The linear trend of the mean annual discharge series (Fig. 10.3) shows a faintly negative slope, which lacks statistical significance. Figure 10.4 shows the mean annual hydrograph for the series of monthly mean discharges (i.e., period of 1943–2018), with maximum discharges occurring during austral spring. The average discharge (i.e., arithmetic mean) for the period was  $47.04 \text{ m}^3 \text{ s}^{-1}$ , whereas the annualized discharge was  $14.84 \text{ km}^3$ , the specific water yield was  $2.87 \text{ L s}^{-1} \text{ km}^{-2}$ , and runoff exceeded  $9 \text{ mm y}^{-1}$ . In this studied time series, instantaneous  $Q_{\max}$  was  $524 \text{ m}^3 \text{ s}^{-1}$ , and  $Q_{\min}$ ,  $2.1 \text{ m}^3 \text{ s}^{-1}$ .

<sup>1</sup>The hydrological data were obtained from the Argentina's Sistema Nacional de Información Hídrica (<https://snih.hidricosargentina.gob.ar/Filtros.aspx>).

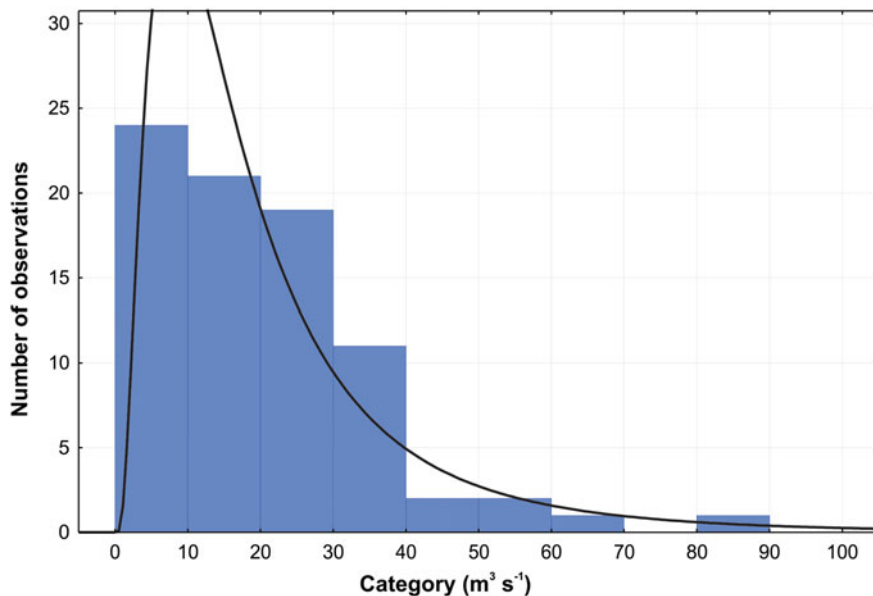


**Fig. 10.2** Log-normal distribution of instantaneous discharges recorded at El Maitén gauging station (2000–2020).  $N = 80$ , chi-square = 7.01392, d.f. = 2,  $p < 0.05$

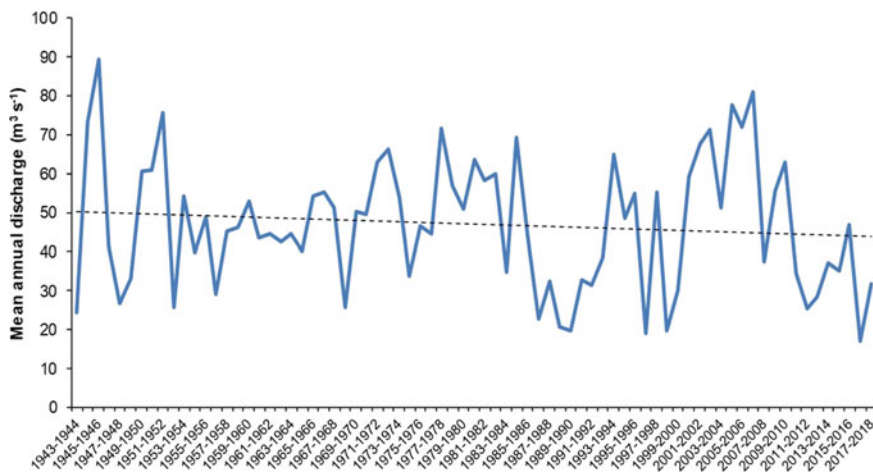


**Fig. 10.3** Mean annual Chubut River discharge time series recorded at Los Altares gauging station during the 1943–2018 time period. The fitted regression line shows a nonsignificant negative trend



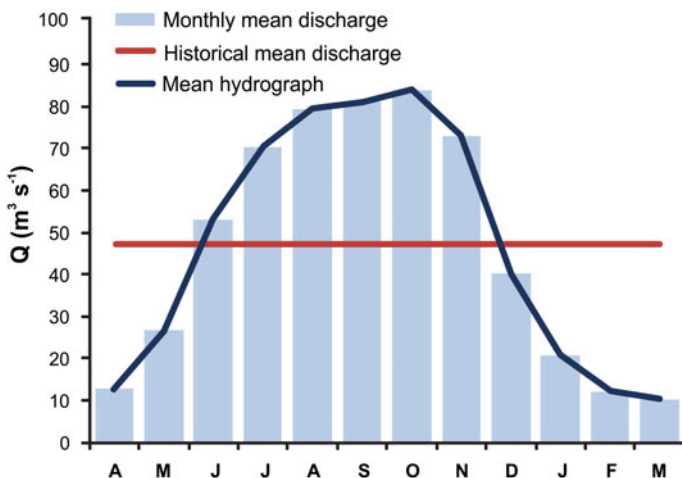


**Fig. 10.4** Historical (1943–2018) mean discharge record at Los Altares, the main stage measuring station at the Chubut River. The graph shows monthly mean discharges, the resulting (arithmetic) mean discharge and the corresponding synthetic hydrograph

As it happens with the upstream discharge time series, the statistical distribution is markedly log-normal. The chi-square test performed to verify log-normality (317.14) exceeds the critical value for 9 degrees of freedom and  $p < 0.001$ . Hence,  $Q_g \pm S_g$  at Los Altares is  $35.9 \pm 2.72 \text{ m}^3 \text{ s}^{-1}$ , which is lower than the arithmetic mean calculated above. The conversion to a Gaussian distribution of the discharge time series (1943–2018) allows to estimate that 95 per cent of the data in the historical discharge series fell within the range  $30.5 < Q_g < 41.4 \text{ m}^3 \text{ s}^{-1}$ .

The seasonal Kendall trend analysis (Kendall 1975; Hirsch et al. 1982) is a nonparametric statistical tool that allows establishing monotonic trends in time series. The use of the technique for the CHR monthly mean discharge time series at Los Altares station (Table 10.1) shows a statistically significant discharge decrease ( $p < 0.05$ ) during January–March and May (i.e., the months with low-water flow).

The Chubut's lower stretch originates at the reservoir lake formed by the Florentino Ameghino dam, which was finished in 1963, 130 km west of the city of Trelew (i.e., Gaiman Department). The reservoir lake has a surface area of  $\sim 70 \text{ km}^2$ , a mean maximum depth of  $\sim 25 \text{ m}$  and a storage capacity of  $\sim 16 \text{ km}^3$  of water, mostly used for irrigation and power generation.

The Valle Inferior ( $43^\circ 17' 35.13'' \text{ S}$ ,  $65^\circ 29' 54.72'' \text{ W}$ ) gauging station is in operation since 1993, and it is located approximately 90 km downstream the Florentino Ameghino dam and less than 50 km upstream from the Chubut's estuary in the Atlantic Ocean. Contrasting with the hydrologic behavior recorded at Los Altares, the annual mean discharge time series (1993–2018 record period) shows a significant decreasing trend, a likely consequence of increased consumptive use and



**Table 10.1** Seasonal Kendall test for the Chubut River monthly mean discharges at Los Altares

	N	Kendall $t$	$p^*$ )
January	75	-2.132	<b>0.01651</b>
February	75	-2.461	<b>0.00693</b>
March	75	-2.159	<b>0.01541</b>
April	75	-0.567	0.28527
May	75	-1.935	<b>0.02649</b>
June	75	-0.814	0.20776
July	75	-0.654	0.25651
August	75	-0.174	0.43100
September	75	0.897	0.18497
October	75	-0.851	0.19743
November	75	-1.505	0.06617
December	75	-1.606	0.05418
Total	900	-1.819	0.03445

\*) Statistically significant parameters in bold ( $p < 0.05$ )

discharge modulation imposed by the dam (Fig. 10.5). In 25 years, annual mean discharges have decreased at a mean rate of  $\sim 10 \text{ m}^3$  per decade. The annual mean discharge (i.e., arithmetic mean) at Valle Inferior is  $34.9 \pm 14 \text{ m}^3 \text{ s}^{-1}$ , whereas the mean annual flow is  $1.1 \text{ km}^3$ . The specific water yield is only  $1.1 \text{ L s}^{-1} \text{ km}^{-2}$ , and runoff is slightly less than  $3.5 \text{ mm y}^{-1}$ . In spite of likely groundwater contributions, the lower reach exhibits a mean discharge which is considerably lower than the one determined in the middle stretch. These hydrological parameters are mostly the after-effect of significant evapotranspiration and the intensive consumptive use of water.

## 10.4 Physical and Chemical Parameters of Surface Water and Groundwater from the Lower Basin of Chubut River

The values of physical and chemical parameters obtained in surface water from CHR in June and November are shown in Fig. 10.6. The temperature ranged from 15.6 to 19.5 °C in spring and from 6.8 to 8.2 °C in winter according to the season. In general, the DO level was close to saturation in both sampled seasons, and the values obtained in winter (98.1–114.3%) were higher than those obtained in spring (81.7–120.2%). The pH was alkaline ranging from 8.0 to 9.0 in both samplings. The EC presented low values ( $330 \mu\text{S cm}^{-1}$ ) in the sites far from the mouth, but it reached a maximum value ( $44,730 \mu\text{S cm}^{-1}$ ) in the estuarine zone evidencing the presence of seawater. Similarly, the TDS showed an increase toward the marine zone, varying from 0.2 to  $29.1 \text{ g L}^{-1}$ . The redox potential presented positive values in all sampling sites and ranged from 169 to 294 mV.

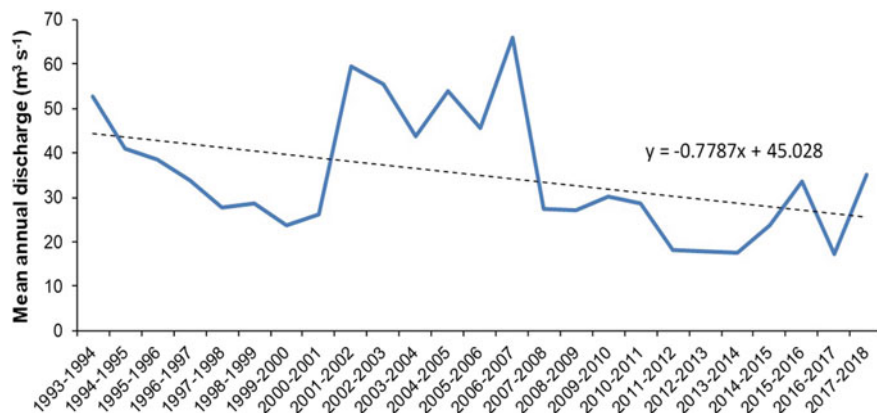


**Fig. 10.5** Mean annual Chubut River discharge time series recorded at Valle Inferior gauging station. The fitted regression line exhibits a statistically significant ( $p < 0.05$ ) trend which shows a mean discharge decrease of  $25 \text{ m}^3$  during the 1993–2018 time period

As expected, groundwater samples exhibited for the same parameters lower values than those found in surface waters (Table 10.2). These parameters varied for DO (42.3–84.3%), temperature (13.7–16.0 °C), EC (638–3351  $\mu\text{S cm}^{-1}$ ), TDS (0.4–2.1  $\text{g L}^{-1}$ ), salinity (0.3–1.7  $\text{g L}^{-1}$ ), pH (6.4–7.6) and redox potential (135–406 mV). Groundwater from the well in the beach (Gw7) and close to the mouth (Gw7) presented lower temperatures, DO and pH, but showed higher EC, salinity and TDS in comparison with CHR surface waters. These values are typical of marine environments suggesting the presence of seawater. Moreover, groundwater samples presented the highest  $^{222}\text{Rn}$  activities. At some sampling sites,  $^{222}\text{Rn}$  activity increased tenfold. Specifically, the Gw7 site presented high  $^{222}\text{Rn}$  activity typical of an underground aquifer, but also presented values of salinity and EC typical of the marine environment. These characteristics are suggesting the presence of a mixing zone between groundwater and seawater.

## 10.5 Dissolved Inorganic Nutrients in Water

In general, CHR surface waters presented lower concentrations of dissolved inorganic nutrients than groundwater (Fig. 10.7 and Table 10.3). In winter, nutrient concentrations were higher than those found in spring but they showed a similar pattern despite the higher water flow in November. Nutrient concentrations varied slightly throughout the studied area, with the exception of the sampling sites 7, 8, 9 and 10, located in the estuarine zone, which exhibited the highest range of variation (Fig. 10.7). In November, the ammonium concentration ranged from 0.35 to 4.75  $\mu\text{M}$ , and the highest value was found at sampling site 7, close to the city of Rawson. This could be associated with the discharge of domestic wastewater into

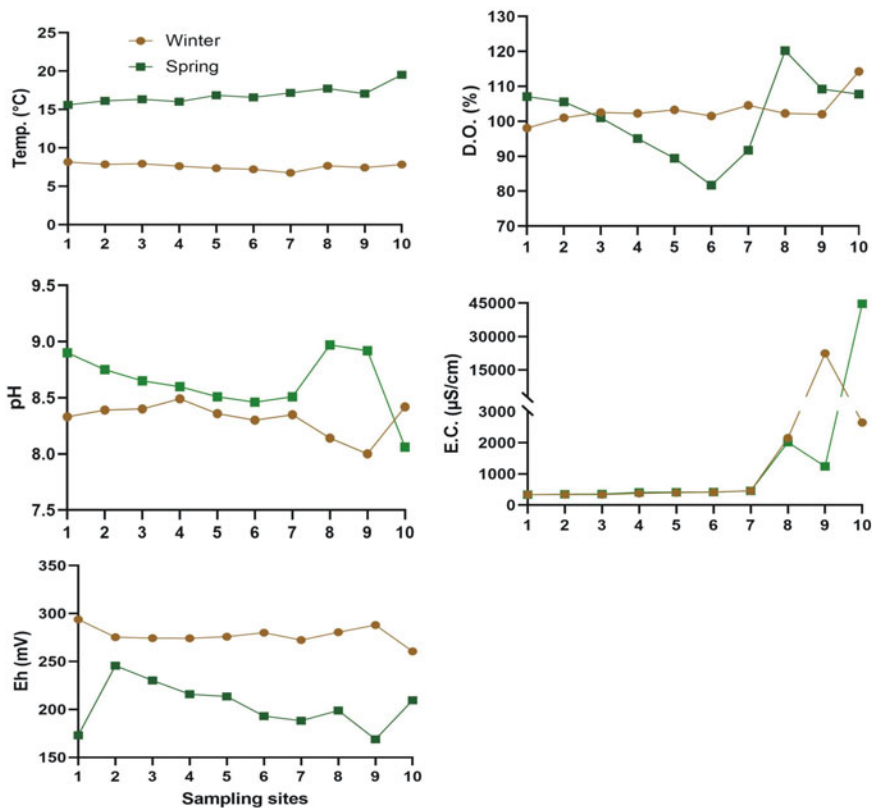


**Fig. 10.6** Physical and chemical parameters measured in situ in surface waters of ten sampling sites located in the lower basin of Chubut River

the CHR. Before being delivered into the river, the residual domestic waters receive a biological treatment which consists of activated sludge and represent an aerobic process. This treatment is efficient to achieve an increase in the clarification of wastewater, but it is difficult to obtain a decrease in nutrient concentrations, mainly of nitrogen and phosphorus. Ammonium through oxidation processes produces nitrate, and this fact could be associated with the maximum of nitrate that was detected upstream in sampling site 7. Considering that nitrogen is the limiting nutrient, both in rivers and in Patagonia’s marine environments (Charpy-Roubaud et al. 1982; Depetris et al. 2005), these nutrients provided by the treatment plant favor the development of primary producers such as those found in the estuarine zone of CHR (Villafañe et al. 1991; Helbling et al. 2010). In addition, nitrate concentrations ranged from 10.2 to 21.9 µM in winter, and the highest value was found at sampling site 8, which is located south of Rawson city, closer to the river mouth. At the same site, the highest phosphate concentration was found, and it varied from 0.5 to 3.6 µM. Finally, the silicic acid concentration ranged from 18.2

**Table 10.2** Physical and chemical parameters measured in Chubut River's surface and bottom waters and in groundwater wells located in the studied area

Site	Temp.	D.O.	E.C.	T.D.S.	Sal.	pH	Eh	<sup>222</sup> Rn	2-Sigma uncert.
	°C	%	μS cm <sup>-1</sup>	g L <sup>-1</sup>	g L <sup>-1</sup>		mV	Dpm L <sup>-1</sup>	Dpm L <sup>-1</sup>
<i>Bottom water (Bw) from Chubut River:</i>									
Bw1	16.4	89.9	313	0.20	0.16	7.8	267	6.0	4.3
Bw2	17.9	107.7	322	0.21	0.14	7.8	283	19.9	6.9
Bw3	17.2	92.4	351	0.23	0.15	7.9	300	9.8	3.5
Bw4	16.0	91.3	409	0.27	0.19	8.6	216	177.4	15.4
Bw5	16.9	93.7	483	0.31	0.21	7.9	262	595.0	30.0
Bw6	15.4	90.3	43,930	28.50	28.57	7.8	324	0.7	1.0
<i>Groundwater (Gw) from well (depth in m)</i>									
Gw1-(20)	13.7	42.3	1822	1.18	0.93	7.4	238	770.4	32.3
Gw2-(30)	15.2	61.8	1038	0.70	0.54	7.4	135	577.6	27.4
Gw3-(60)	16.0	60.5	638	0.41	0.31	7.6	229	584.7	30.1
Gw4-(6)	15.5	64.4	3351	2.18	1.74	7.6	164	237.5	6.1
Gw5-(7)	13.9	47.6	807	0.66	0.51	6.4	406	444.8	33.4
Gw6-(3)	15.0	42.8	670	0.50	0.40	7.5	152	886.7	39.0
Gw7-(18)	15.1	84.3	33,686	26.10	25.70	8.6	149	237.2	19.9
Gw8-(1)	13.3	79.2	32,225	26.90	26.60	7.1	205	111.7	13.7

The number in parentheses indicates the depth of well

to 261.5 μM, and the highest values were found at sampling sites far from the mouth, while the lowest concentration was found at sampling site 10, close to the marine zone. Silicic acid presented concentrations that were two orders of magnitude higher than other nutrients in the investigated river reach. Due to its distribution pattern, it is widely used as a proxy to estimate the continental contribution to the coastal marine zone. In general, with exception of the silicic acid, nutrient concentrations increased toward the CHR's mouth.

As expected, concentrations of dissolved inorganic nutrients in groundwater were higher than in surface waters of the CHR (Table 10.3). In this sense, the ammonium and phosphate concentrations were an order of magnitude higher, and nitrate concentrations were two orders of magnitude higher than those found in surface waters. In addition, ammonium concentration reached 37.1 μM in a well (Gw7) located in a fishing plant close to the estuarine zone. This concentration is seven times higher than that found in surface waters of the CHR. The phosphate concentration reached 28.8 μM, and it was eight times higher than the concentration recorded in surface water. The nitrate concentration ranged from 1.1 to 683.3 μM, and it was fifty-eight times higher than those measured in surface waters. Similar to surface waters, groundwater presented an increase in nutrient

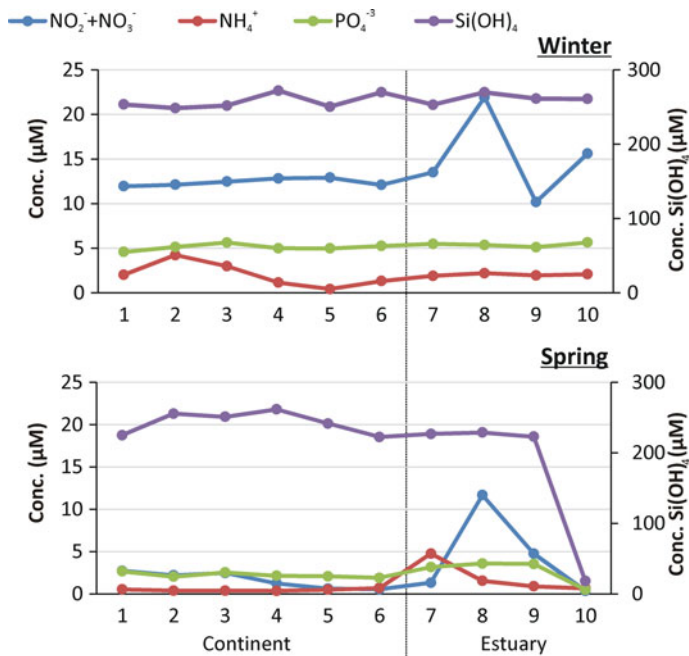


**Fig. 10.7** Concentrations of dissolved inorganic nutrients in surface waters in ten sampling sites of the lower basin of the Chubut River in winter (up) and spring (down). Vertical line indicates the limit of seawater intrusion according to Perillo et al. (1989)

concentrations toward the estuarine zone. The silicic acid concentrations in groundwaters were 2.6 times higher and of the same order of magnitude than those registered in surface water. They ranged from 325 to 699 μM, with the exception of the sampling site Gw8 located close to the beach area, which presented a value of 16.1 μM, suggesting a dilution effect caused by the intrusion of the seawater.

### 10.5.1 Estimation of the Monthly Nutrient Flux

Considering the nutrient concentrations and river discharge, it is possible to estimate the flow of chemical substances transported by the river during the sampling time interval. Using discrete samples, an instant estimation of river contribution to the ocean was obtained. In this case, the load values for each sampling site were calculated using the nutrient concentration and the water discharge at each specific point (GESAMP 1987).

**Table 10.3** Concentrations of dissolved inorganic nutrients ( $\mu\text{M}$ ) in bottom waters from the Chubut River and groundwater from wells located in the lower basin of Chubut River. N/D: No detectable

<i>Groundwater (Gw) from well</i>				
Site/ nutrient	Ammonium	Nitrate	Phosphate	Silicic acid
Gw1	0.1	26.1	N/D	556.8
Gw2	0.4	17.4	0.1	624.8
Gw3	0.1	56.5	N/D	471.9
Gw4	N/D	22.9	5.0	653.9
Gw5	1.0	288.3	4.8	699.0
Gw6	0.8	362.0	17.4	550.2
Gw7	37.1	683.3	28.8	325.6
Gw8	77.3	1.1	16.0	16.8
<i>Bottom water (Bw) from Chubut River</i>				
Bw1	0.9	<0.1	1.2	113.3
Bw2	1.9	<0.1	0.9	119.5
Bw3	3.2	0.1	1.4	136.5
Bw4	2.6	1.2	2.1	144.8
Bw5	1.2	3.4	1.6	157.4
Bw6	1.5	3.3	1.3	27.3

The CHR-estimated nutrient flux toward the coastal marine zone was higher in June than in November (Table 10.4). Additionally, the total inorganic nitrogen (TIN) was higher than inorganic phosphorus. However, the silicic acid loads were the largest and they were an order of magnitude higher than the loads of nitrogen and phosphorus. Due to this fact, and also because this nutrient is mostly originated from a natural source, silicic acid flow is used as a tracer of riverine discharge.

In winter, the flow rate from the dam is lower than the spring discharge due to the fact that there is no snowmelt in the mountain region. In spring, there is an increase in the flow rate favored by the beginning of thawing. However, this water is less enriched in nutrient than those that drain during winter. Defrosting increases  $\text{Si}(\text{OH})_4$  concentration and, to a lesser extent, the nitrogen and phosphorous concentrations. In addition, there is a higher water demand during this season due to increased agricultural activities, which are carried out mainly in the proximities of three cities which are placed furthest from the estuarine zone (i.e., in the area of sampling sites 1–5).

At sampling site 8, there is a marked increase in the load of  $\text{N-NO}_3^-$  in both sampling campaigns. This seems to be unrelated to the river discharge, and it could be caused by the discharge into the CHR of domestic wastewater from the city of Rawson. On the contrary, this nutrient load was reduced to one-half during the sampling campaign carried out in November, probably due to the dilution effect caused by higher discharge. Clearly, the strong increase of  $\text{N-NO}_3^-$  load in this site is caused by anthropogenic activities from urban settlements. In winter,  $\text{PO}_4^{3-}$  loads were similar in all sampling sites. In November, the highest loads were detected at

**Table 10.4** Nutrient loads ( $\text{t month}^{-1}$ ) obtained in each sampling site along the Chubut River in June and November

June						November				
Flow rate from dam: $46.89 \text{ m}^3 \text{ s}^{-1}$						Flow rate from dam: $51.36 \text{ m}^3 \text{ s}^{-1}$				
Site	N-NH <sub>4</sub> <sup>+</sup>	N-NO <sub>3</sub> <sup>-</sup>	TIN	PO <sub>4</sub> <sup>-3</sup>	Si(OH) <sub>4</sub>	N-NH <sub>4</sub> <sup>+</sup>	N-NO <sub>3</sub> <sup>-</sup>	TIN	PO <sub>4</sub> <sup>-3</sup>	Si(OH) <sub>4</sub>
1	3.7	22.3	26	18.9	947.8	0.9	4.8	5.7	10.3	793.1
2	7.9	22.6	30.5	21.2	929.6	0.7	3.9	4.5	7.9	900.8
3	5.5	23.3	28.8	23.2	941.8	0.7	4.3	5	9.8	885.1
4	2.1	23.9	26	20.6	1017.3	0.6	2.2	2.8	8.3	922.2
5	0.8	24.1	24.8	20.5	936.3	0.9	1.1	2	8.1	851.2
6	2.5	22.6	25	21.6	1008.6	1.2	0.9	2.1	7.3	784.2
7	3.5	25.2	28.7	22.6	945.9	8.3	2.3	10.7	12.3	799.7
8	4.1	40.9	45	22.1	1008.7	2.7	20.5	23.2	13.9	806.5
9	3.6	19	22.6	21.1	977.4	1.6	8.3	9.9	13.7	785.7
10	3.9	29.1	33	23.3	975.3	1.1	0.6	1.7	1.9	64.2

the sampling sites located near the estuarine zone. This behavior could be similar to that described by Niencheski et al. (1999), who suggested that  $\text{PO}_4^{-3}$  is removed from the water column from Patos Lagoon estuary in the lower salinity region (less than ca.  $10 \text{ g L}^{-1}$ ) and released at salinities above ca.  $10 \text{ g L}^{-1}$ . On the case of CHR, the release for the water column would occur at lower salinity region, that is, where happens the transition from the fluvial to estuarine conditions.

Silicic acid, followed by nitrogen and then phosphate were the main nutrients delivered by the CHR into Engaño Bay. These nutrient loads are consistent but lower than those reported by Helbling et al. (1992) for the CHR in the periods 1986 and 1987. Other studies have recognized that the CHR has noteworthy N-NO<sub>3</sub><sup>-</sup> concentrations, which is surely determined by human contribution such as the mesotrophic Florentino Ameghino dam, farmlands and the cities located in the lowermost stretch (Depetris et al. 2005). These authors have determined the nutrient fluxes from Patagonia's rivers that are discharged into the coastline. In addition, these authors have estimated for the CHR fluxes of silicic acid ( $1075 \text{ t month}^{-1}$ ), nitrate ( $93 \text{ t month}^{-1}$ ) and phosphate ( $28 \text{ t month}^{-1}$ ) which are the same order of magnitude as those obtained in this study (Table 10.4). On the other hand, the application of models demonstrated that dam-modulated rivers produce an increase of 10% in the nitrogen flux and a reduction of 25 and 30% in the  $\text{Si(OH)}_4$  and  $\text{PO}_4^{-3}$  fluxes, respectively, in comparison with undammed rivers (Sferratore et al. 2008). Nitrogen is the limiting nutrient for phytoplankton production in the Patagonia's marine environments (Charpy-Roubaud et al. 1982). In consequence, these contributions of nutrients are important because they fertilize the estuarine zone (Helbling et al. 1992), sustaining phytoplankton production (Villafañe et al. 1991), which is crucial for the marine food web.



## 10.6 Groundwater Contribution to the Lower Chubut River

Surface waters of CHR showed variable  $^{222}\text{Rn}$  activities (Table 10.5). In general, lower  $^{222}\text{Rn}$  was detected in the upstream sampling points (from 48 to 331  $\text{Bq m}^{-3}$ ), whereas at sampling sites Bw4 and Bw5, higher  $^{222}\text{Rn}$  concentrations were recorded (from 569 to 1770  $\text{Bq m}^{-3}$ ). The sampling point located near the river outflow into the Atlantic Ocean (sampling point Bw6) showed the lowest  $^{222}\text{Rn}$  activity ( $\sim 9 \text{ Bq m}^{-3}$ ) due to marine intrusion. Based on  $^{222}\text{Rn}$  concentrations, two groundwater end members were defined:  $C_{g1} = 12,752 \text{ Bq m}^{-3}$  and  $C_{g2} = 7412 \text{ Bq m}^{-3}$  (Table 10.5).

The contribution of groundwater into the lower stretch of the Chubut River—with the exception of sampling point Bw6—was estimated by means of a  $^{222}\text{Rn}$  mass balance equation proposed by Hamada (1999):

$$Q_g = \frac{C_2 Q_2 - C_1 Q_1 \exp(-aL)}{\frac{C_g (1 - \exp(-aL))}{aL}}$$

where  $Q_g$  is the groundwater inflow ( $\text{m}^3 \text{ s}^{-1}$ );  $C_1$  and  $C_2$  are the  $^{222}\text{Rn}$  concentrations in river water at the upstream and downstream stations ( $\text{Bq m}^{-3}$ ), respectively;  $Q_1$  and  $Q_2$  are the river discharges at the upstream and downstream stations ( $\text{m}^3 \text{ s}^{-1}$ ), respectively;  $C_g$  is the  $^{222}\text{Rn}$  concentration in groundwater ( $\text{Bq m}^{-3}$ );  $L$  is the distance between stations (km); and  $a$  is a parameter that can be calculated using the following equation:

$$a = (D/zhv) + (\lambda/v)$$

where  $D$  is the molecular diffusivity of  $^{222}\text{Rn}$ , which has been defined by Peng et al. (1974) as a function of temperature  $D = 10^{-(980/(T+273)+1.59)}$  ( $1 \times 10^{-5} \text{ m}^2 \text{ s}^{-1}$  at 25 °C);  $z$  is the thickness of a stagnant film (m), which is about 20  $\mu\text{m}$  when the distance between stations is several kilometers (Hamada et al. 1997);  $h$  is the average stream depth (m);  $v$  is the average stream velocity ( $\text{m s}^{-1}$ ); and  $\lambda$  is the  $^{222}\text{Rn}$  decay constant ( $2.08 \times 10^{-6} \text{ s}^{-1}$ ).

The values of the parameters employed in the  $^{222}\text{Rn}$  mass balance calculation are listed in Table 10.5, as well as the calculated groundwater contribution. Results indicate that the groundwater inflow to the river is low at sampling point Bw2 ( $Q_g = 2.03 \text{ m}^3 \text{ s}^{-1}$ ), whereas a negative value was obtained at sampling point Bw3 ( $Q_g = -1.32 \text{ m}^3 \text{ s}^{-1}$ ), which suggests that at this location the river is losing water to the aquifers through the streambed. Groundwater inflow slightly increases downstream at sampling point Bw4 ( $Q_g = 2.31 \text{ m}^3 \text{ s}^{-1}$ ), while the highest groundwater discharge was detected at sampling point Bw5 ( $Q_g = 5.41 \text{ m}^3 \text{ s}^{-1}$ ). Thus, the  $^{222}\text{Rn}$  mass balance indicates that groundwater inputs may account for about 6–8.5% of the total water inputs to CHR upstream Gaiman city, whereas it increases downstream, reaching  $\sim 24\%$  at Trelew city.

**Table 10.5**  $^{222}\text{Rn}$  activities measured in bottom waters from Chubut River and groundwater end members, parameters used in the mass balance equation and calculated groundwater discharge to the lower Chubut River

Sample	$C^{222}\text{Rn}$	Q	h	v	L	$Qg$ ( $\text{m}^3 \text{s}^{-1}$ )	
	( $\text{Bq m}^{-3}$ )	( $\text{m}^3 \text{s}^{-1}$ )	(m)	( $\text{m s}^{-1}$ )	(m)	G1	G2
Bw1	48.0	26.40	2.0	0.55			
Bw2	331.3	32.49	2.5	0.52	310	0.74	1.28
Bw3	162.5	27.65	3.0	0.42	26,980	-0.49	-0.83
Bw4	569.5	26.74	3.1	0.36	25,900	0.85	1.46
Bw5	1770.0	22.74	2.5	0.40	24,930	1.99	3.42
Bw6	8.7	–	–	–	–	–	–
G1	12,752	–	–	–	–	–	–
G2	7,412	–	–	–	–	–	–

High concentrations of  $^{222}\text{Rn}$  are present in the waters of the CHR only in the immediate vicinity of groundwater advection points and for relatively short distances downstream from such locations. Although high activity of  $^{222}\text{Rn}$  was observed in waters collected near the bottom, low concentrations of nutrients were detected. This was contrary to our expectations. We assume that the nutrients provided by groundwater are immediately affected by the dilution process with fresh surface waters. To confirm this hypothesis, it is necessary to use appropriate equipment to obtain the water sample at the sediment–water column interface, such as the use of benthic chambers or corers (Niencheski and Jahnke 2002). For this reason, the concentrations of nutrients associated with the groundwater that advect toward the CHR have not been sampled conveniently to indicate that the bottom water is more concentrated than the surface water. However, despite this, for the boxes (A, C, D, E) where the advection of groundwater was determined, the contributions of TIN, phosphate and silicic acid for groundwater were 3.6%, 3.4% and 6.6%, respectively, in relation to freshwater. Another factor to be considered is that the mass balance model applied in this study is considered as a site of advection, only the small area that refers to the riverbed.

As indicated by Torres et al. (2018),  $^{222}\text{Rn}$  is a useful tracer in this Patagonian environment, showing water flowing across the sediment–water interface and into the overlying water column, regardless of its composition. It is necessary to expand these data sets to include riverine freshwater, terrestrial groundwater and saline, and recirculated seawater to better understand and quantify this important process in this particular stretch of CHR's coastal region, where the hydraulic gradient certainly is the main driving force that results in freshwater and terrestrial aquifer water discharging at the coastline.

In this particular region of CHR outflow into Engaño Bay, other driving forces that control recirculated seawater are very significant, such as tidal pumping and wave setup. We suggest that measurements of radon isotopes should continue, in both high-resolution time series and horizontal offshore transects, to allow

quantifying the offshore transport rates of discharged continental groundwater. Considering that the SGD has important implications in the biogeochemical cycles of coastal environments, future studies in this region should complement isotopic measurements with determinations of inorganic nutrients, iron, carbon, rare earth elements and toxic metals. Furthermore, we suggest reducing the distance between sampling sites where bottom waters were taken in order to detect other sites with groundwater advection.

## 10.7 Estimation of Nutrient Mass Balance

A mass balance model was applied in the lower basin of the CHR, in order to detect the movement and inputs of nutrients in several sections. For the mass balance calculations, the CHR was divided into eight boxes (Fig. 10.1). This division was made according to the surrounding land use, the existence of urban settlements, anthropogenic impact, the location of sampling stations and the identification of the halocline inside the river. Boxes A and H represent the highest and lowest parts of the catchment, respectively. In the area encompassed around boxes A to E, strong agricultural and livestock breeding activities are developed. The largest city (Trelew) in the drainage basin is located in box F. Rawson, the capital city of Chubut Province, is located in box G. The presence of seawater has been identified strongly in box H and weakly in box G, which results in a mixing process producing modifications in the physical and chemical characteristics during the transition from the riverine environment to Engaño Bay, where marine conditions are finally reached.

For each box, the plot of the excess or deficit was integrated over the study period to estimate the net excess or deficiency of each nutrient in the estuary. The difference between the observed total content and the calculated total content of nutrients for each of the boxes in both sampling campaigns is plotted in Fig. 10.8. Only the silicic acid and TIN are presented. The excesses (values >0) and deficits (values <0) of each nutrient varied according to the box. These results were adjusted from both spatial and temporal points of view. In general, the maximum excesses were recorded in the boxes near to the mouth with exception for the  $\text{Si(OH)}_4$ .

Regarding the spatial variation, in winter, the mass balance of nitrogen compounds,  $\text{PO}_4^{3-}$  and  $\text{Si(OH)}_4$  was positive in the estuarine zone (boxes G and H). This indicates that the CHR is discharging these nutrients into the marine coastal zone. Moreover, the high nutrient concentrations found in surface waters could suggest that the CHR receives nutrients such as nitrogen and phosphorus from external sources and silicic acid associated with sediment transport or groundwater. The evident riverine contribution of nutrients could be related mainly to the discharge of domestic wastewater from the city of Rawson. The wastewater inflow to rivers is the main problem caused by anthropogenic activities that take place in the coastline, thus stimulating the eutrophication of such aquatic environments. Soils are not the

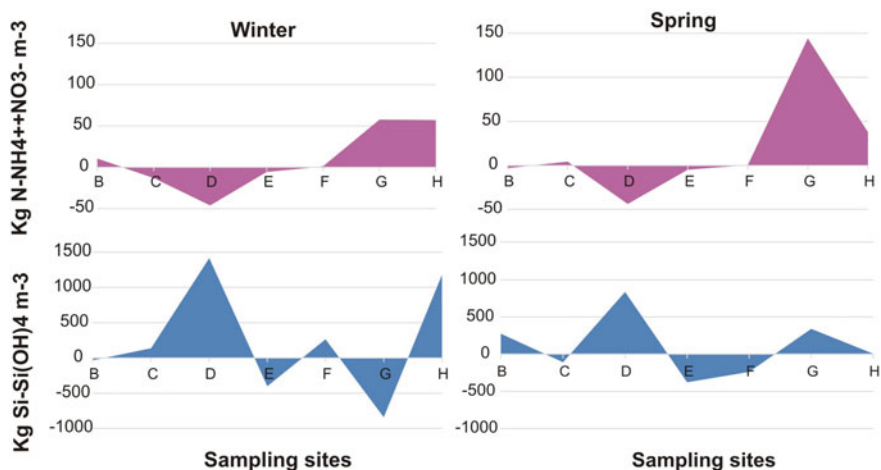


**Fig. 10.8** Difference between the observed total content and the calculated total content (excess or deficit) for TIN and silicic acid in each of the seven boxes in winter (left) and spring (right)

only important source of nitrate and ammonium to the hydrosphere; additionally, nitrogen enters the river mainly through rain and porewater from the sediment (Depetris et al. 2005). Given the low rainfall prevailing in the region, their contribution is scarce, and more attention should be paid to the contribution from the sediment. In addition, the region suffers the indiscriminate use of fertilizers and pesticides in agricultural activities which are strongly developed and also represent —along with livestock— the main economic activity. Although this region is undergoing pollution originating in anthropogenic activities, its impact has not yet been measured. On the other hand, the distribution of the  $\text{Si(OH)}_4$  also presented excesses in box D (Gaiman) which could be associated with the high density of human-made channels that extract freshwater from the riverbed for irrigation and the leftover is then returned downstream, thus favoring the increase of this nutrient. Since seawater presents low concentrations, the sources of  $\text{Si(OH)}_4$  are the river and groundwater. Furthermore, urban pollution has no influence on its concentration.

In spring, TIN and  $\text{PO}_4^{-3}$  presented the same distribution pattern in each of the boxes. The main excesses in boxes G and H could be associated with domestic wastewater discharges from Rawson city (Fig. 10.8). Also, a marked deficit for both nutrients was found in box D (Fig. 10.8).

Regarding the observed temporal variation, all measured nutrients presented in winter and spring the same distribution pattern and, in both cases, the highest excesses were registered in the estuarine zone (boxes G and H), thus indicating a strong supply of nutrients from the CHR into the marine zone. Specifically, the CHR contributes more  $\text{N-NO}_3^-$  than  $\text{N-NH}_4^+$  into Engaño Bay. Contrarily, the domestic sewages are characterized by containing higher  $\text{N-NH}_4^+$  than  $\text{N-NO}_3^-$  concentration. However,  $\text{N-NH}_4^+$  can produce  $\text{N-NO}_3^-$  by a nitrification process before it reaches the sea. Furthermore, there are some fish-processing plants located

on the margin of the CHR which discharge their industrial wastewater without previous or with inefficient treatment. When these nutrients reach the marine zone, they are incorporated by macroalgae which have a higher assimilation rate of  $\text{N-NH}_4^+$  than  $\text{N-NO}_3^-$  (Torres et al. 2004; Gil et al. 2005). In addition, the  $\text{Si(OH)}_4$  present in both samplings showed a marked increase in box D, which is located in the region irrigated by means of an extended channel network. In this way, they would be delivering a significant amount of this nutrient into the river. On the other hand, the residence time (not shown) was estimated for each box and significant differences were not observed between the two different sampling campaigns.

The analysis of the riverine nutrient supply to Engaño Bay was performed by taking into account only the nutrient concentrations in box H during winter because during this sampling excursion the highest nutrient concentrations were found. The total nutrient inputs are shown in Table 10.6.

During the winter season, the amount of  $\text{Si(OH)}_4$  discharged into the Engaño Bay area was two orders of magnitude higher than nitrogen (as TIN) and  $\text{PO}_4^{3-}$ . The total amounts of nutrient reported in this study were lower than those noted by Helbling et al. (1992) in 1986 and 1987. In addition, in the estuarine low salinity zone the patches of diatoms *Aulacoseira granulata* (Ehr.) Simonsen and *Odontella aurita* (Lyngbye) Agardh are accompanied by extreme fluctuations in chlorophyll *a* concentrations, from less than 5 to  $45 \mu\text{g L}^{-1}$  (Villafañe et al. 1991). However, although information on phytoplankton primary production levels is lacking, we can estimate the potential production rate sustained by the nitrogen flux from CHR (Table 10.6) applying a Redfield ratio of C106:Si15:N16:P1 for diatoms (Redfield et al. 1963) and the total N flux in the CHR's box H. Thus, a nitrogen flux of  $0.08 \times 10^6 \text{ mol day}^{-1}$  would support a production rate of  $7.42 \times 10^6 \text{ g C day}^{-1}$ . This rate is considered lower than those obtained for Patos Lagoon of  $1.9 \times 10^8 \text{ g C day}^{-1}$  (Niencheski et al. 2007). These results are consistent if one bears in mind that the freshwater discharge into the sea at Los Patos Lagoon is two orders of magnitude higher than CHR. A comparison with the total amount of nutrients discharged by CHR into Engaño Bay shows that it is several orders of magnitude lower than other world rivers (Helbling et al. 1992).

## 10.8 Conclusions

The seasonal trend analysis allowed determining a historical discharge decrease during the dry season (i.e., January–March and May). The high nutrient concentrations (mainly N and P) found in surface water reflect the contributions of urban wastewater from coastal cities, hence being the more evident anthropogenic impact near the mouth of the CHR, while silicic acid is associated with natural processes such as sediment transport and advection of groundwater. The  $^{222}\text{Rn}$  concentration recorded in bottom waters from CHR is suggesting the presence of groundwater by a molecular diffusion process. The  $^{222}\text{Rn}$  concentrations along the CHR changed spatially between the town of 28 de Julio and Trelew city suggesting the presence

**Table 10.6** Estimated nutrient fluxes to the Engaño Bay from Chubut River at box H

Nutrient	$10^6 \text{ mol day}^{-1}$
N-NH <sub>4</sub> <sup>+</sup>	0.009
N-NO <sub>3</sub> <sup>-</sup>	0.07
N-TIN	0.08
P-PO <sub>4</sub> <sup>-3</sup>	0.024
Si-Si(OH) <sub>4</sub>	1.175

of the groundwater. The <sup>222</sup>Rn mass balance allowed identifying areas of the river with low <sup>222</sup>Rn activities indicating that CHR is losing water to the aquifers and other areas with high <sup>222</sup>Rn activities, which are assumed to be zones where groundwater discharge into CHR is significant. Future studies should take into account performing <sup>222</sup>Rn time series in CHR throughout an entire tidal cycle to determine the effect known as “tidal pump” on SGD. Furthermore, considering that SGD interferes in the biogeochemical cycles of micro- and macro-elements we suggest performing chemical measurements in waters from the estuarine zone. Finally, we consider it relevant to perform measurements of Ra and Rn isotopes along with transects perpendicular to the coast of Engaño Bay, which will allow quantifying the transport rate of SGD. These activities must be carried out at different seasons in order to detect the variability between the wet and dry seasons.

**Acknowledgements** The authors wish to thank the staff of the FURG’s Laboratory of Hydrochemical (Brazil); Córdoba National University (Argentina); CICTERRA-CONICET (Argentina); and Chemical Oceanography and Water Pollution Laboratory (LOQyCA) of CESIMAR—CCT CONICET—CENPAT (Argentina). This study was partially funded by the Bilateral Cooperation Project between Argentina’s CONICET and Brazil’s CAPES (Project BR/RED 1302) which involved the aforementioned institutions. We wish to thank D. -P. Häder for the editorial suggestions and the anonymous reviewer for the constructive comments that improved the manuscript.

## References

- Antolini L (2012) Percepción del riesgo y dinámica de uso de plaguicidas agrícolas en el Valle Inferior del Río Chubut. Rawson. 1. Ministerio de Salud Argentina, Technical report, 183pp
- Bratton JF (2010) The three scales of submarine groundwater flow and discharge across passive continental margins. *J Geol* 118:565–575. <https://doi.org/10.1086/655114>
- Burnett W, Cable J, Corbett D, Chanton J (1996) Tracing groundwater flow into surface waters using natural <sup>222</sup>Rn. In: Buddemeier R (ed) *Groundwater Discharge in the Coastal Zone: Proceedings of an International Symposium*. LOICZ IGBP. LOICZ/R&S/96-8, iv + 179pp. LOICZ, Texel, The Netherlands, pp 22–28
- Burnett WC, Bokuniewicz H, Huettel M, Moore WS, Taniguchi M (2003) Groundwater and pore water inputs to the coastal zone. *Biogeochemistry* 66:3–33. <https://doi.org/10.1023/B:BIOG.0000006066.21240.53>

- Burnett WC, Dulaiova H (2003) Estimating the dynamics of groundwater input into the coastal zone via continuous radon-222 measurements. *J Environ Radioact* 69:21–35. [https://doi.org/10.1016/S0265-931X\(03\)00084-5](https://doi.org/10.1016/S0265-931X(03)00084-5)
- Campodonico VA, García MG, Pasquini AI (2015) The dissolved chemical and isotopic signature downflow the confluence of two large rivers: The case of the Parana and Paraguay rivers. *J Hydrol* 528:161–176. <https://doi.org/10.1016/j.jhydrol.2015.06.027>
- Cecil LD, Green JR (2000) Radon-222. In: Cook PG (ed) *Environmental tracers in subsurface hydrology*. Springer US, Boston, MA, pp 175–194
- Charpy-Roubaud CJ, Charpy LJ, Maestrini SY (1982) Fertilité des eaux côtières nord-patagoniques: facteurs limitant la production du phytoplancton et potentialités d'exploitation mycicole. *Oceanol Acta* 5(2):179–188
- Comendatore M, Esteves J (2004) Natural and anthropogenic hydrocarbons in sediments from the Chubut River (Patagonia, Argentina). *Mar Pollut Bull* 48:910–918. <https://doi.org/10.1016/j.marpolbul.2003.11.015>
- Davis J (1986) *Statistics and data analysis in geology*. Wiley, New York
- Depetris PJ, Gaiero DM, Probst JL, Hartmann J, Kempe S (2005) Biogeochemical output and typology of rivers draining Patagonia's Atlantic seaboard. *J Coast Res* 21(4):835–844. <https://doi.org/10.2112/015-NIS.1>
- EMC. Estación Meteorológica Cenpat (2020) <http://repositorio.cenpat-conicet.gob.ar:8081/xmliui/handle/123456789/400>. Accessed 10 Sep 2020
- García-Solsona E, García-Orellana J, Masqué P, Garcés E, Radakovitch O, Mayer A, Estradé E, Basterretxea G (2010) An assessment of karstic submarine groundwater and associated nutrient discharge to a Mediterranean coastal area (Balearic Islands, Spain) using radium isotopes. *Biogeochemistry* 97:211–229
- GESAMP (1987) *Land/Sea Boundary Flux of Contaminants: Contributions from Rivers*. UNESCO/GESAMP Report and Studies N<sup>o</sup>. 32, 172pp
- Gil MN, Harvey MA, Esteves JL (1999) Heavy metals in intertidal surface sediments from the Patagonian coast, Argentina. *Bull Environ Contam Toxicol* 63:52–58. <https://doi.org/10.1007/s001289900947>
- Gil MN, Torres AI, Esteves JL (2005) Uptake of sewage derived nitrogen by *Ulva rigida* (Chlorophyceae) in Bahía Nueva (Golfo Nuevo, Patagonia, Argentina). *Hydrobiologia* 39–43
- Godoy JM, Souza TA, Godoy MLDP, Moreira I, Carvalho ZL, Lacerda LD, Fernandes FC (2013) Groundwater and surface water quality in a coastal bay with negligible fresh groundwater discharge: Arraial do Cabo, Brazil. *Mar Chem* 156:85–97. <https://doi.org/10.1016/j.marchem.2013.05.004>
- Hamada H (1999) Analysis of the interaction between surface water and groundwater using radon-222. *Japan Agric Res Q* 33:261–265
- Hamada H (2000) Estimation of groundwater flow rate using the decay of Rn-222 in a well. *J Environ Radioact* 47:1–13
- Hamada H, Imaizumi M, Komae T (1997) Methods of investigation and analysis on ground-water using radon as an indicator. *Nat Res Inst Agric Eng* 36:17–50
- Helbling WE, Pérez DE, Medina CD, Lagunas MG, Villafañe VE (2010) Phytoplankton distribution and photosynthesis dynamics in the Chubut River estuary (Patagonia, Argentina) throughout tidal cycles. *Limnol Oceanogr* 55:55–65. <https://doi.org/10.4319/lo.2010.55.1.0055>
- Helbling WE, Santamarina JM, Villafañe VE (1992) Chubut River Estuary (Argentina): Estuarine variability under different conditions of river discharge. *Rev Biol Mar Oceanogr* 27:73–90
- Hirsch RM, Slack JR, Smith RA (1982) Techniques of trend analysis for monthly water quality data. *Water Resour Res* 18:107–121. <https://doi.org/10.1029/WR018i001p00107>
- Kendall M (1975) *Rank correlation methods*. Griffin, London
- Kroeger KD, Charette MA (2008) Submarine groundwater discharge: nitrogen biogeochemistry of the discharge zone. *Limnol Oceanogr* 53:1025–1039
- Kwon EY, Kim G, Primeau F, Moore WS, Cho HM, Devries T, Sarmiento JL, Charette MA, Cho YK (2014) Global estimate of submarine groundwater discharge based on an



- observationally constrained radium isotope model. *Geophys Res Lett* 41:8438–8444. <https://doi.org/10.1002/2014GL061574>
- Macheleidt W, Nestler W, Grischek T (2002) Determination of hydraulic boundary conditions for the interaction between surface water and groundwater. *Geol Soc Publ* 193(1):235–243
- Milliman J, Farnsworth K (2011) *River discharge to the coastal ocean: a global synthesis*. Cambridge University, Cambridge
- Moore WS (1999) The subterranean estuary: a reaction zone of ground water and sea water. *Mar Chem* 65:111–125
- Moore WS (2006) Radium isotopes as tracers of submarine groundwater discharge in Sicily. *Cont Shelf Res* 26:852–861
- Niencheski LF, Baumgarten M da G, Fillmann G, Windom HL (1999) Nutrients and suspended matter behaviour in the Patos Lagoon Estuary (Brazil). In: Perillo G, Piccolo MC, Pino-Quivira M (eds) *Estuaries of South America their geomorphology and dynamics*. Springer, Berlin Heidelberg, pp 67–81
- Niencheski LF, Jahnke RA (2002) Benthic respiration and inorganic nutrient fluxes in the estuarine region of Patos Lagoon (Brazil). *Aquat Geochemistry* 8:135–152. <https://doi.org/10.1023/A:1024207220266>
- Niencheski LFH, Windom HL, Moore WS, Jahnke RA (2007) Submarine groundwater discharge of nutrients to the ocean along a coastal lagoon barrier, Southern Brazil. *Mar Chem* 106:546–561. <https://doi.org/10.1016/j.marchem.2007.06.004>
- Paparazzo F, Crespi-Abril A, Gonçalves R, Barbieri ES, Gracia Villalobos LL, Solís ME, Soria G (2018) Patagonian dust as a source of macronutrients in the Southwest Atlantic Ocean. *Oceanography* 31:33–39. <https://doi.org/10.5670/oceanog.2018.408>
- Peng TH, Takahashi T, Broecker WS (1974) Surface radon measurements in the North Pacific Ocean station Papa. *J Geophys Res* 79:1772–1780
- Perillo G, Piccolo MC, Scapini M del C, Orfila J (1989) Hydrography and circulation of the Chubut river estuary (Argentina). *Estuaries* 12:186–194
- Peterson RN, Santos IR, Burnett WC (2010) Evaluating groundwater discharge to tidal rivers based on a Rn-222 time-series approach. *Estuar Coast Shelf Sci* 86:165–178. <https://doi.org/10.1016/j.ecss.2009.10.022>
- Porcelli D, Swarzenski PW (2003) The behaviour of U- and Th series nuclides in groundwater. *Rev Mineral Geochemistry* 52:317–361
- Redfield AC, Ketchum BH, Richard FA (1963) The influence of organisms on the composition of seawater. In: Hill MN (ed) *The sea*, vol 2. Wiley, New York
- Santos IR, Dimova N, Peterson RN, Mwashote B, Chanton J, Burnett WC (2009) Extended time series measurements of submarine groundwater discharge tracers ( $^{222}\text{Rn}$  and  $\text{CH}_4$ ) at a coastal site in Florida. *Mar Chem* 113:137–147. <https://doi.org/10.1016/j.marchem.2009.01.009>
- Santos IR, Eyre BD, Huettel M (2012) The driving forces of porewater and groundwater flow in permeable coastal sediments: a review. *Estuar Coast Shelf Sci* 98:1–15
- Schmidt C, Hanfland C, Regnier P, Van Cappellen P, Schluter M, Knauth U, Stimac I, Geibert W (2011)  $^{228}\text{Ra}$ ,  $^{226}\text{Ra}$ ,  $^{224}\text{Ra}$  and  $^{223}\text{Ra}$  in potential sources and sinks of land-derived material in the German Bight of the North Sea: implications for the use of radium as a tracer. *Geo-Marine Lett* 31:259–269. <https://doi.org/10.1007/s00367-011-0231-5>
- Sferratore A, Billen G, Garnier J, Smedberg E, Humborg C, Rahm L (2008) Modelling nutrient fluxes from sub-arctic basins: comparison of pristine vs. dammed rivers. *J Mar Syst* 73:236–249. <https://doi.org/10.1016/j.jmarsys.2007.10.012>
- Skalar Analytical® VB (2005a) Skalar methods—analysis: Nitrate + Nitrite—Catnr. 461-031 +DIAMOND Issue 081505/MH/99235956. Breda, The Netherlands
- Skalar Analytical® VB (2005b) Skalar methods—analysis: Phosphate—Catnr. 503-010w/r +DIAMOND Issue 081505/MH/99235956. Breda, The Netherlands
- Skalar Analytical® VB (2005c) Skalar methods—analysis: Silicate—Catnr. 563-051 + DIAMOND Issue 081505/MH/99235956. Breda, The Netherlands

- Smerdon BD, Payton Gardner W, Harrington GA, Tickell SJ (2012) Identifying the contribution of regional groundwater to the baseflow of a tropical river (Daly River, Australia). *J Hydrol* 464–465:107–115. <https://doi.org/10.1016/j.jhydrol.2012.06.058>
- Strickland JDH, Parsons TR (1972) A practical handbook of the seawater analysis, 2nd edn. Fisheries Research Board of Canada Bulletin No 157, 310p
- Stringer CE, Burnett WC (2004) Sample bottle design improvements for radon emanation analysis of natural waters. *Heal Phys* 87:642–646
- Swarzenski PW, Burnett WC, Greenwood WJ, Herut B, Peterson R, Dimova N, Shalem Y, Yechieli Y, Weinstein Y (2006) Combined time-series resistivity and geochemical tracer techniques to examine submarine groundwater discharge at Dor Beach, Israel. *Geophys Res Lett* 33:L24405. <https://doi.org/10.1029/2006GL028282>
- Swarzenski PW, Dulai H, Kroeger KD, Smith CG, Dimova N, Storlazzi CD, Prouty NG, Gingerich SB, Glenn CR (2017) Observations of nearshore groundwater discharge: Kahekili Beach Park submarine springs, Maui, Hawaii. *J Hydrol Reg Stud* 11:147–165. <https://doi.org/10.1016/j.ejrh.2015.12.056>
- Torres AI, Andrade CF, Moore WS, Faleschini M, Esteves JL, Niencheski LFH, Depetris PJ (2018) Ra and Rn isotopes as natural tracers of submarine groundwater discharge in the Patagonian coastal zone (Argentina): an initial assessment. *Environ Earth Sci* 77:145–155. <https://doi.org/10.1007/s12665-018-7308-7>
- Torres AI, Gil MN, Esteves JL (2004) Nutrient uptake rates by the alien alga *Undaria pinnatifida* (Phaeophyta) (Nuevo Gulf, Patagonia, Argentina) when exposed to diluted sewage effluent. *Hydrobiologia* 520:1–6
- Villafañe VE, Helbling WE, Santamarina JM (1991) Phytoplankton blooms in the Chubut River estuary (Argentina): influence of stratification and salinity. *Rev Biol Mar Oceanogr* 26:1–20
- Windom HL, Moore WS, Niencheski LFH, Jahnke RA (2006) Submarine groundwater discharge: a large, previously unrecognized source of dissolved iron to the South Atlantic Ocean. *Mar Chem* 102:252–266. <https://doi.org/10.1016/j.marchem.2006.06.016>